Mixing of X and Y states from QCD sum rules analysis*

Ze-Sheng Chen(陈泽升)[1] Zhuo-Ran Huang(黄卓然)[2] Hong-Ying Jin(金洪英)[1†]
T.G. Steele[3] Zhu-Feng Zhang(张珠峰)[4]

[1]Institute of Modern Physics, Department of Physics, Zhejiang University, Hangzhou 310027,China
[2]Institute of High Energy Physics, Chinese Academy of Sciences, Beijing 100049, China
[3]Department of Physics and Engineering Physics, University of Saskatchewan, Saskatoon, Saskatchewan, S7N 5E2, Canada
[4]Department of Physics, Ningbo University, Ningbo 315211, China

Abstract: We study $\bar{Q}Q\bar{q}q$ and $\bar{Q}q\bar{Q}q$ states as mixed states in QCD sum rules. By calculating the two-point correlation functions of pure states of their corresponding currents, we review the mass and coupling constant predictions of $J^{PC}=1^{++}$, 1^{--}, and 1^{-+} states. By calculating the two-point mixed correlation functions of $\bar{Q}Q\bar{q}q$ and $\bar{Q}q\bar{Q}q$ currents, we estimate the mass and coupling constants of the corresponding "physical state" that couples to both $\bar{Q}Q\bar{q}q$ and $\bar{Q}q\bar{Q}q$ currents. Our results suggest that for 1^{++} states, the $\bar{Q}Q\bar{q}q$ and $\bar{Q}q\bar{Q}q$ components are more likely to mix, while for 1^{--} and 1^{-+} states, there is less mixing between $\bar{Q}Q\bar{q}q$ and $\bar{Q}q\bar{Q}q$. Our results suggest the Y series of states have more complicated components.

Keywords: four-quark states, QCD sum rules, non-perturbative QCD

DOI: 10.1088/1674-1137/ac531a

I. INTRODUCTION

In 2003, Belle observed a new state known as $X(3872)$, which definitely contained a charm-anticharm pair and could not be explained by the ordinary quark-antiquark model [1]. Since then, more new hadrons containing heavy quarks have been found and studied in numerous experiments [2]. These hadrons are known as XYZ states, which contain a heavy quark-antiquark pair and at least a light quark-antiquark pair; they are naturally exotics [3]. Many structures have been proposed to describe XYZ states that include molecular, tetraquark, and hybrid components [4–6]. Like the studies of other mesons with exotic quantum numbers, convincing explanations of the observed XYZ states remain an open question in phenomenological particle physics. Recently, a study of $X(3872)$ by LHCb argued that the compact component should be required in X states [7]; this result is more likely to support the tetraquark model of XYZ states but not exclude the molecular model of all exotic states. In this paper, we focus on the states in two simple $\bar{Q}q\bar{Q}q$ and $\bar{Q}Q\bar{q}q$ combinations to study XYZ states ($\bar{Q}$ represents a heavy c or b quark, while q represents a light u,d or s quark). These two forms have been extensively studied previously [8, 9]. However, $\bar{Q}q\bar{Q}q$ and $\bar{Q}Q\bar{q}q$ states are difficult to distinguish straightforwardly from the decay modes of XYZ states because XYZ states are usually observed to have both $\bar{Q}Q+\bar{q}q$ like decay modes and $\bar{Q}q+Q\bar{q}$ like decay modes. Many scenarios were studied to qualitatively distinguish $\bar{Q}q\bar{Q}q$ and $\bar{Q}Q\bar{q}q$ states [10–14]. Furthermore, the physical states are usually mixtures of different structures, and this makes the problem more complicated. In a previous study we have developed a method to estimate the mixing strength of different currents from a QCD sum rule (QCDSR) approach [15–18]; we use the same technique to study the mixing of $\bar{Q}q\bar{Q}q$ and $\bar{Q}Q\bar{q}q$ XY states.

In this study, we investigated three kinds of vector states with different quantum numbers $J^{PC}=1^{++}$, 1^{--}, 1^{-+}. These states have long been considered to be $\bar{Q}q\bar{Q}q$ or $\bar{Q}Q\bar{q}q$ molecular states in different studies [19–25]. However, since many of them have abundant decay modes, mixing scenarios should be taken into account. Besides, it is generally believed that there is a large background of two free mesons spectrum in the two points correlation function of four-quark currents. To avoid such a large uncertainty, it is especially important to estimate the mixing strength of $\bar{Q}q\bar{Q}q$ and $\bar{Q}Q\bar{q}q$ currents to investigate the corresponding physical states. The calculations will show us whether the physical states prefer to be

Received 13 December 2021; Accepted 9 February 2022; Published online 11 April 2022
* Supported by NSFC (11175153, 11205093) and the Natural Sciences and Engineering Research Council of Canada (NSERC)
† E-mail: jinhongying@zju.edu.cn

$\bar{Q}q\bar{Q}\bar{q}$ or $\bar{Q}Q\bar{q}q$ molecular states, or whether they are strongly mixed states.

As mentioned above, for the 1^{++} channel, $X(3872)$ has been extensively studied for a wide variety of structures [26, 27]. In molecular state schemes, $X(3872)$ has been usually considered a D^*D molecular state [12– 14]. However, although the pure D^*D molecular state was predicted to have a mass close to $X(3872)$, it had too large a decay width to agree with the experimental results [28, 29]. Moreover, the $J/\psi\rho$ and $J/\psi\omega$ states have a similar mass, since the sum of the masses of their two constituent parts are close to $X(3872)$. Hence, the mixing of these two molecular states is naturally possible. Furthermore, in a recent observation of $X(3872)$ by LHCb [7], the compact component was found to be required. Hence, we will consider another state $\bar{c}c$ in the mixing; this has been studied in [28].

For the 1^{--} channel, many 1^{--} states are found in the range of 4200 –4700 MeV, permitting an abundance of possible pure or mixed molecular states. Some 1^{--} states have very similar masses like $Y(4220)/Y(4260)$ and $Y(4360)/Y(4390)$ [30, 31]. Hence, it is interesting and meaningful to investigate the possible mixing of molecular states, which has not been previously studied.

For 1^{-+} sector, no confirmed heavy hadrons with 1^{-+} quantum numbers have been observed. Some potential candidates include $X(3940)$, $X(4160)$, $X(4350)$ [2]. The constructions of 1^{-+} molecular states in the $\bar{Q}q\bar{Q}\bar{q}$ and $\bar{Q}Q\bar{q}q$ scenarios are possible. As outlined below, we calculate the mass spectrum of these states and estimate their mixing strength in both the u,d and s quark cases to help guide searches for these states in the 1^{-+} sector.

Our methodology is introduced in Section II. Then, we discuss the 1^{++} states, 1^{--} states, and 1^{-+} states in Sections III, IV, and V, respectively. We discuss the importance of non-perturbative terms in calculations that evaluate the mixing strength in Section VI. Finally, we present our summary and conclusions in the last section.

II. QCDSR APPROACH AND MIXING STRENGTH

In QCDSR, we normally construct a mixing current that combine two state interpretations. The two-point correlation function of the mixing currents can be written as

$$\begin{aligned}\Pi(q^2) =& \mathrm{i}\int \mathrm{d}^4x\,\mathrm{e}^{\mathrm{i}qx}\left\langle 0\left|T\left\{(j_a(x)+cj_b(x))(j_a^+(0)+cj_b^+(0))\right\}\right|0\right\rangle \\ =&\Pi_a(q^2)+2c\Pi_{ab}(q^2)+c^2\Pi_b(q^2),\end{aligned} \tag{1}$$

where j_a and j_b have the same quantum numbers; c is a real parameter related to the mixing strength (not the mixing strength itself, since c may not been normalized), and

$$\begin{aligned}\Pi_a(q^2) =& \mathrm{i}\int \mathrm{d}^4x\,\mathrm{e}^{\mathrm{i}qx}\left\langle 0\left|T(j_a(x)j_a^+(0))\right|0\right\rangle, \\ \Pi_b(q^2) =& \mathrm{i}\int \mathrm{d}^4x\,\mathrm{e}^{\mathrm{i}qx}\left\langle 0\left|T(j_b(x)j_b^+(0))\right|0\right\rangle, \\ \Pi_{ab}(q^2) =& \frac{\mathrm{i}}{2}\int \mathrm{d}^4x\,\mathrm{e}^{\mathrm{i}qx}\left\langle 0\left|T(j_a(x)j_b^+(0)+j_b(x)j_a^+(0))\right|0\right\rangle.\end{aligned} \tag{2}$$

Here, we consider the mixed correlator Π_{ab} because it provides a signal that indicates which states couple to both currents. One can insert a complete set of particle eigenstates between j_a and j_b, and the state with a relatively strong coupling to both these currents will be selected out through the QCDSR. By estimating the mass and coupling constants as well as taking experimental results into account, one can obtain insight into the constituent composition of the corresponding states. This method worked well in our previous study on vector and scalar meson states [15] and has been successfully applied in other systems [16–18].

Π_{ab} usually can be decomposed into a different Lorentz structure

$$\Pi_{ab}(q^2) = \sum_n \Pi_n(q^2)A_n, \tag{3}$$

where $n = 1,2,3...$, $\Pi_n(q^2)$ is the mixing state correlation function with specific quantum numbers, and A_n is the corresponding Lorentz structure. The forms of A_n are related to j_a and j_b, and we will define them in the sections below. For simplicity, we assume a specific $\Pi_H(q^2)$ represents a mixed-state correlation function and is one of the possible $\Pi_n(q^2)$. We also assume that $\Pi_H(q^2)$ obeys the dispersion relation [32]

$$\Pi_H(q^2) = \int_{s_{\min}}^{\infty} \mathrm{d}s\frac{\rho_H(s)}{s-q^2-\mathrm{i}\epsilon}+\ldots, \tag{4}$$

where the spectral density $\rho_H(s) = \frac{1}{\pi}\mathrm{Im}\Pi_H(s)$, $s_{\min}$ represents the physical threshold of the corresponding current, and the dots on the right hand side represent the polynomial subtraction terms to render $\Pi_H(q^2)$ finite. The spectral density $\rho_H(s)$ can be calculated using the operator product expansion (OPE). In this paper, we calculate the spectral density $\rho_H(s)$ up to dimension-six operators,

$$\begin{aligned}\rho_H^{(\mathrm{OPE})}(s) =& \rho_H^{(\mathrm{pert})}(s)+\rho_H^{\langle\bar{q}q\rangle}(s)+\rho_H^{\langle G^2\rangle}(s) \\ &+\rho_H^{\langle\bar{q}Gq\rangle}(s)+\rho_H^{\langle\bar{q}q\rangle^2}(s)+\ldots,\end{aligned} \tag{5}$$

then

$$\Pi_H^{(\mathrm{OPE})}(q^2) = \int_{s_{\min}}^{\infty} \mathrm{d}s \frac{\rho_H^{(\mathrm{OPE})}(s)}{s - q^2 - \mathrm{i}\epsilon} + \ldots . \tag{6}$$

On the phenomenological side, by using the narrow resonance spectral density model,

$$\Pi_H^{(\mathrm{phen})}(q^2) = \frac{\lambda_a \lambda_b^* + \lambda_b \lambda_a^*}{2} \frac{1}{M_H^2 - q^2} + \int_{s_0}^{\infty} \mathrm{d}s \frac{\rho_H^{(\mathrm{cont})}(s)}{s - q^2 - \mathrm{i}\epsilon}, \tag{7}$$

where λ_a and λ_b are the respective couplings of the ground state to the corresponding currents; M_H represents the mass of the mixed state, which has relatively strong coupling to the corresponding currents; $\rho_H^{(\mathrm{cont})}$ represents continuum contributions to spectral density, and s_0 is the continuum threshold. By using the QCDSR continuum spectral density assumptions

$$\rho_H^{(\mathrm{cont})}(s) = \rho_H^{(\mathrm{OPE})}(s)\Theta(s - s_0), \tag{8}$$

and equating the OPE side and the phenomenological side of the correlation function, $\Pi_H^{(\mathrm{phen})}(q^2) = \Pi_H^{(\mathrm{OPE})}(q^2)$, we obtain the QCDSR master equation

$$\int_{s_{\min}}^{s_0} \mathrm{d}s \frac{\rho_H^{(\mathrm{OPE})}(s)}{s - q^2 - \mathrm{i}\epsilon} + \ldots = \frac{\lambda_a \lambda_b^* + \lambda_b \lambda_a^*}{2} \frac{1}{M_H^2 - q^2}. \tag{9}$$

After applying the Borel transformation operator $\hat{B}$ to both sides of the master equation, the subtraction terms are eliminated, and the master equation can be written as [32, 33]

$$\int_{s_{\min}}^{s_0} \mathrm{d}s \rho_H^{(\mathrm{OPE})}(s) \mathrm{e}^{-s\tau} = \frac{\lambda_a \lambda_b^* + \lambda_a^* \lambda_b}{2} \mathrm{e}^{-M_H^2 \tau}, \tag{10}$$

where the Borel parameter $\tau = 1/M^2$, and M is the Borel mass. The master equation (10) is the foundation of our analysis. By taking the τ logarithmic derivative of Eq. (10), we obtain

$$M_H^2 = \frac{\int_{s_{\min}}^{\infty} \mathrm{d}s\, s\rho_H^{(\mathrm{OPE})}(s) \mathrm{e}^{-s\tau}}{\int_{s_{\min}}^{\infty} \mathrm{d}s\, \rho_H^{(\mathrm{OPE})}(s) \mathrm{e}^{-s\tau}}. \tag{11}$$

One can set $a = b$ in Eqs. (7), (9), and (10) to obtain the original pure state QCDSR.

Eq. (10) is not valid for all values of τ because of the OPE truncation and the simplified assumption for the phenomenological spectral density; thus, the determination of the sum rule window, in which the validity of (10) can be established, is very important. In the literature, different methods are used in the determination of the τ sum rule window [34, 35]. In this paper, we follow similar previous studies to restrict the resonance and high dimension condensate contributions (HDC), i.e., the resonance part obeys the relation

$$\frac{\int_{s_{\min}}^{s_0} \mathrm{d}s\, \rho_H^{(\mathrm{OPE})}(s) \mathrm{e}^{-s\tau}}{\int_{s_{\min}}^{\infty} \mathrm{d}s\, \rho_H^{(\mathrm{OPE})}(s) \mathrm{e}^{-s\tau}} > 40\%, \tag{12}$$

while HDC (usually $\langle\bar{q}q\rangle^2$ in molecular systems) obeys the relation

$$\frac{|\int_{s_{\min}}^{\infty} \mathrm{d}s\, \rho_H^{\langle\bar{q}q\rangle^2}(s) \mathrm{e}^{-s\tau}|}{|\int_{s_{\min}}^{\infty} \mathrm{d}s\, \rho_H^{(\mathrm{OPE})}(s) \mathrm{e}^{-s\tau}|} < 10\%. \tag{13}$$

Furthermore, the value of s_0 is also very important in QCDSR methods. It is often assumed that the threshold satisfies $\sqrt{s_0} = M_H + \Delta_s$, with $\Delta_s \approx 0.5$ GeV. This is especially the case in molecular state QCDSR calculations [36, 37].

The approximation $\sqrt{s_0} = M_H + \Delta_s$ can be understood in QCDSR because the parameter s_0 separates the ground state and other excited states' contributions to spectral density. Hence, one can set s_0 less than the first excitation threshold in the case of involving excited state contributions in the spectral density, and Δ_s represents the approximate mass difference between the ground and first excited states. We assume that the first excited state is approximately equal to an excited constituent meson and another ground state constituent meson. Then, we can establish s_0 by comparing the mass difference between the ground constituent meson and the first excited constituent meson of the corresponding state (like the charmonium and D meson family in our case). We have listed some experimental data for the charmonium and D meson families in Table 1 and Table 2. One can easily find that the mass difference between the ground state and first excited state are all around $0.5^{+0.1}_{-0.1}$ GeV, and the fluctuations are all acceptable in the QCDSR approach.

In order to estimate the mixing strength of the physical state strongly coupled to both of the two different currents, we define

Table 1. Charmed meson ($c = \pm 1$) states, where q represents the u,d quark. The • symbol indicates particles that have confirmed quantum numbers.

PDG name	Possible structure	Ground state	Possible 1st excited state	Δ_s/MeV
D	$\bar{c}\gamma_5 q$	•$D(1865)$	$D(2550)$	~685
D_1	$\bar{c}\gamma_\mu\gamma_5 q$	•$D_1(2420)$	–	–
D_0^*	$\bar{c}q$	•$D_0^*(2300)$	$D_J^*(2600)$	~300
D^*	$\bar{c}\gamma_\mu q$	•$D^*(2007)$	$D^*(2640)$	~633

Table 2. Charmonium (possibly non-$\bar{c}c$ states). The • symbol indicates particles that have confirmed quantum numbers.

Possible structure	Ground state/MeV	Possible 1st excited state/MeV	Δ_s/MeV
$\bar{c}\gamma_5 c$	$\bullet\eta_c(1S)$/2984	$\bullet\eta_c(2S)$/3637	~653
$\bar{c}\gamma_\mu\gamma_5 c$	$\bullet\chi_{c1}(1P)$/3510	$\bullet\chi_{c1}(3872)$	~362
$\bar{c}c$	$\bullet\chi_{c0}(1P)$/3415	$\chi_{c0}(3860)$	~445
$\bar{c}\gamma_\mu c$	$\bullet J/\psi(1S)$/3097	$\bullet\psi(2S)$/3686	~589

$$N \equiv \frac{|\lambda_a\lambda_b^* + \lambda_a^*\lambda_b|}{2|\lambda_a'\lambda_b'|}, \tag{14}$$

where λ_a' and λ_b' are coupling constants of the relevant current with a pure state (i.e., the coupling that emerges in the diagonal correlation functions Π_a, Π_b). Eq. (14) is analogous to the mixing parameter defined in Ref. [38]. By using appropriate factors of mass in the definitions of λ_a' and λ_b', we can compare the magnitude of coupling constants and estimate the mixing strength self-consistently. The mixing strength depends on the definition and normalization of the mixed state. For example, in Ref. [39] the definition of the mixed state is

$$|M\rangle = \cos\theta|A\rangle + \sin\theta|B\rangle, \tag{15}$$

where $|M\rangle$ is a mixed state composed of pure states $|A\rangle$ and $|B\rangle$, and θ is a mixing angle. In this definition and normalization of the mixed state, we see that $N \approx \cos\theta\sin\theta$, and $N \in \left(0, \frac{1}{2}\right)$. We use Eq. (14) as a robust parameter to quantify mixing effects because of the different possible normalizations and mixed state definitions. Furthermore, because the behavior of N is not linear, we define $\widetilde{N}$ under the scenario of Eq. (15):

$$\widetilde{N} = \sin^2\left(\frac{\arcsin(2N)}{2}\right). \tag{16}$$

The quantity $\widetilde{N}$ gives the approximate proportion of the pure part of the mixed state. A comparison of the the mixed state mass with the two relevant pure states suggests that the mixed state is dominated by the part whose pure state mass prediction is the closest to the mixed state mass. Different decay widths can also help us to distinguish the dominant part of the mixed state.

We use the following numerical values of vacuum condensates consistent with other QCDSR analyses of XYZ states: $\langle\bar{q}q\rangle = (-0.23\pm0.03)^3$ GeV^3, $\langle\bar{q}g_s\sigma Gq\rangle = m_0^2\langle\bar{q}q\rangle$, $m_0^2 = 0.8$ GeV^2, $\langle\alpha_s G^2\rangle = 0.07\pm0.02$ GeV^4, and $\langle\bar{s}s\rangle = (0.8\pm0.2)\langle\bar{q}q\rangle$ [40, 41]. In addition, the quark masses $m_c = 1.27$ GeV, $m_q = \frac{1}{2}(m_u + m_d) = 0.004$ GeV, and $m_s = 0.096$ GeV, at the energy scale $\mu = 2$ GeV [2], are used.

III. MIXED STATE IN 1^{++} CHANNEL

We start from the following three forms of currents:

$$\begin{aligned}
j_{\mu\nu}^{X_A}(x) =& \frac{\mathrm{i}}{\sqrt{2}}[\bar{c}(x)\gamma_\mu c(x)\bar{q}(x)\gamma_\nu q(x) \\
&- \bar{c}(x)\gamma_\nu c(x)\bar{q}(x)\gamma_\mu q(x)], \\
j_\mu^{X_{B_1}}(x) =& \frac{\mathrm{i}}{\sqrt{2}}[\bar{c}(x)\gamma_\mu q(x)\bar{q}(x)\gamma_5 c(x) \\
&- \bar{q}(x)\gamma_\mu c(x)\bar{c}(x)\gamma_5 q(x)], \\
j_\mu^{X_{B_2}}(x) =& \frac{\mathrm{i}}{\sqrt{2}}[\bar{c}(x)\gamma_\mu\gamma_5 q(x)\bar{q}(x)c(x) \\
&+ \bar{q}(x)\gamma_\mu\gamma_5 c(x)\bar{c}(x)q(x)], \\
j_\mu^{X_C}(x) =& \frac{1}{6\sqrt{2}}\langle\bar{q}q\rangle\bar{c}(x)\gamma_\mu\gamma_5 c(x),
\end{aligned} \tag{17}$$

where X denotes the 1^{++} state, the subscript A of X denotes the $\bar{Q}Q\bar{q}q$ scenario, B denotes the $\bar{Q}qQ\bar{q}$ scenario, C denotes the $\bar{Q}Q$ scenario, and the corresponding mesonic structures of these currents are listed in Table 3. We note that the former two currents can be decomposed into two constituent meson currents, and the mass prediction of each corresponding pure state are usually close to the sum of the masses of these two constituent mesons. The current $j_{\mu\nu}^{X_A}$ can be decomposed into $J/\psi(1S)(3097)$ and $\rho(770)$ currents; $j_\mu^{X_{B_1}}(x)$ can be decomposed into $D^*(2007)$ and $D(1865)$ currents. The sums of the masses of the two constituent mesons are both close to $X(3872)$. Hence, we choose these two currents to study $X(3872)$. The current $j_\mu^{X_{B_2}}$ has the same quantum numbers, and it cannot be excluded in 1^{++} mixing state structures. Besides, $j_\mu^{X_C}(x)$ is normalized according to Ref. [28]. Since the mixing between $j_\mu^{X_C}(x)$ and $\bar{Q}Q\bar{q}q$ is suppressed ($\bar{q}q$ in $\bar{Q}Q\bar{q}q$ becomes a bubble and vanishes), we only consider the mixing between $j_\mu^{X_C}(x)$ and $j_\mu^{X_{B_1}}(x)$ or $j_\mu^{X_{B_2}}(x)$.

To study the pure $\bar{Q}Q\bar{q}q$, $\bar{Q}q\bar{Q}q$, and $\bar{Q}Q$ states, the respective two-point correlation functions can be decomposed into different Lorentz structures.

$$\begin{aligned}
\Pi_{\mu\nu\rho\sigma}^{X_A}(q^2) =& \Pi_a^{X_A}(q^2)\frac{1}{q^2}(q^2 g_{\mu\rho}g_{\nu\sigma} - q^2 g_{\mu\sigma}g_{\nu\rho} \\
&- q_\mu q_\rho g_{\nu\sigma} + q_\mu q_\sigma g_{\nu\rho} - q_\nu q_\sigma g_{\mu\rho} + q_\nu q_\rho g_{\mu\sigma}) \\
&+ \Pi_b^{X_A}(q^2)\frac{1}{q^2}(-q_\mu q_\rho g_{\nu\sigma} + q_\mu q_\sigma g_{\nu\rho} \\
&- q_\nu q_\sigma g_{\mu\rho} + q_\nu q_\rho g_{\mu\sigma}), \\
\Pi_{\mu\nu}^{X_{B_k}/C}(q^2) =& \Pi_{(1)}^{X_{B_k}/C}(q^2)\left(-g_{\mu\nu} + \frac{q_\mu q_\nu}{q^2}\right) \\
&+ \Pi_{(0)}^{X_{B_k}/C}(q^2)\left(\frac{q_\mu q_\nu}{q^2}\right),
\end{aligned} \tag{18}$$

Table 3. Summary of results for 1^{++} states. $\lambda = \frac{\lambda_a\lambda_b^*+\lambda_a^*\lambda_b}{2}$ when mixed cases are involved, the same below.

State	Current structure	Mass/GeV	$\lambda/10^{-4}$ GeV^{10}	$\sqrt{s_0}$/GeV	τ window/GeV^{-2}
X_A	$J/\psi\rho$	$3.798^{+0.09}_{-0.09}$	$1.49^{+0.51}_{-0.47}$	4.4	0.30 – 0.31
X_{B_1}	$D^*\bar{D}$	$3.857^{+0.06}_{-0.06}$	$2.24^{+0.65}_{-0.53}$	4.4	0.31 – 0.39
X_{B_2}	$D_1\bar{D}_0^*$	$5.310^{+0.04}_{-0.04}$	$69.0^{+15.0}_{-14.0}$	5.8	0.20 – 0.29
X_C	χ_{c1}	$3.511^{+0.02}_{-0.03}$	$0.0229^{+0.0017}_{-0.0018}$	4.5	0.29 – 0.31
M_{X_1}	$J/\psi\rho$ - $D^*\bar{D}$	$3.987^{+0.06}_{-0.06}$	$0.168^{+0.049}_{-0.042}$ GeV^{-1}	4.4	0.30 – 0.32
M_{X_2}	$J/\psi\rho$ – $D_1\bar{D}_0^*$	$4.945^{+0.08}_{-0.06}$	$0.760^{+0.29}_{-0.20}$ GeV^{-1}	5.45	0.22 – 0.24
M_C	χ_{c1} - $D^*\bar{D}$	$3.818^{+0.03}_{-0.02}$	$0.0282^{+0.0027}_{-0.0024}$	4.5	0.28 – 0.30

where $k=1,2$; $\Pi_a^{X_A}$ and $\Pi_b^{X_A}$ describe the pure molecular state contribution with respective quantum numbers 1^{++} and 1^{-+}; and $\Pi_{(1)}^{X_{B_k}/C}$ and $\Pi_{(0)}^{X_{B_k}/C}$ describe 1^{++} and 0^{-+} state contributions, respectively. In the mixing scenario, we start from the off-diagonal mixed correlator described in the previous section, i.e.,

$$\begin{aligned}\Pi_{\mu\nu\sigma}^{M_{X_1}}(q^2) =& \frac{\mathrm{i}}{2}\int \mathrm{d}^4x\mathrm{e}^{\mathrm{i}q\cdot x}\langle 0|T(j_{\mu\nu}^{X_A}(x)j_\sigma^{X_{B_1}+}(0)\\ &+ j_\sigma^{X_{B_1}}(x)j_{\mu\nu}^{X_A+}(0))|0\rangle,\\ \Pi_{\mu\nu\sigma}^{M_{X_2}}(q^2) =& \frac{\mathrm{i}}{2}\int \mathrm{d}^4x\mathrm{e}^{\mathrm{i}q\cdot x}\langle 0|T(j_{\mu\nu}^{X_A}(x)j_\sigma^{X_{B_2}+}(0)\\ &+ j_\sigma^{X_{B_2}}(x)j_{\mu\nu}^{X_A+}(0))|0\rangle,\end{aligned} \tag{19}$$

where M_{X_k}, $k=1,2$, are mixed states assumed to result from the corresponding currents. These mixed correlators have the Lorentz structure

$$\Pi_{\mu\nu\sigma}^{M_{X_k}}(q^2) = \Pi^{M_{X_k}}(q^2)(q_\alpha\epsilon_{\alpha\mu\nu\sigma}). \tag{20}$$

Furthermore, when we consider the two-quark states $j_\mu^{X_C}(x)$, the mixed correlator and its Lorentz structure are

$$\begin{aligned}\Pi_{\mu\nu}^{M_C}(q^2) =& \frac{\mathrm{i}}{2}\int \mathrm{d}^4x\mathrm{e}^{\mathrm{i}q\cdot x}\langle 0|T(j_\mu^{X_C}(x)j_\nu^{X_{B_1}+}(0)\\ &+ j_\nu^{X_{B_1}}(x)j_\mu^{X_C+}(0))|0\rangle,\\ \Pi_{\mu\nu}^{M_C}(q^2) =& \Pi_{(1)}^{M_C}(q^2)\left(-g_{\mu\nu}+\frac{q_\mu q_\nu}{q^2}\right)+\Pi_{(0)}^{M_C}(q^2)\left(\frac{q_\mu q_\nu}{q^2}\right),\end{aligned} \tag{21}$$

where $\Pi_{(1)}^C$ and $\Pi_{(0)}^C$ describe the 1^{++} and 0^{-+} state contributions, respectively. Here, we just consider the state mixed with $j_\mu^{X_C}$ and $j^{X_{B_1}}$; this state is a candidate for $X(3872)$.

We follow the 40%–10% sum-rule window and Δ_s methods mentioned in Section II. After establishing the τ window by the 40%–10% method at a specific s_0, we use Eq. (11) for each state to plot the τ behavior of M_H for the chosen s_0 (see Appendix A for details). The mass prediction M_H and s_0 are then compared with the constraint $\sqrt{s_0} = M_H + \Delta_s$. Then, s_0 is adjusted, and the analysis is repeated until we find the best (M_H, s_0) solutions that satisfy the relation $\sqrt{s_0} = M_H + \Delta_s$. The coupling constants are naturally obtained through the predicted M_H and s_0 according to Eq. (10). The mass and coupling constant prediction and associated QCDSR parameters are presented in Table 3. All the parameters are the average values in the corresponding τ window.

The uncertainties are mainly from the input parameters. For instance, $\langle\alpha_s G^2\rangle = 0.07\pm0.02$ GeV^4, $\langle\bar{s}s\rangle = (0.8\pm0.2)\langle\bar{q}q\rangle$, and $\langle\bar{q}q\rangle = (-0.23\pm0.03)^3$ GeV^3. The quark masses and other parameters included in the calculations have uncertainties of less than 5% due to substantial numerical fittings by other researchers. There is also an uncertainty about the value of the threshold s_0. Analogous to the studies in Refs. [20, 42], the fluctuation of threshold is set to be ±0.1 GeV($\sqrt{s_0}$).

In the pure state calculations, a τ window of $X_A(3798)$ state cannot be determined under 40%–10% and the Δ_s method, and we rearrange the limits of resonance and HDC to 35%–15% (one may naturally expect that the pure-state analysis requires such adjustments because of mixing). The states $X_A(3798)$ and $X_{B_1}(3857)$ both have mass predictions close to $X(3872)$. However, the large mass prediction of the $X_{B_2}(5310)$ state is far beyond the D_1+D_0^* threshold, and does not match the observed 1^{++} states.

The mixing strength can then be estimated by computing the value of N via Eq. (14). Note that the coupling constants of the two mixed state correlators have the form

$$\begin{aligned}\Pi_{\mu\nu\sigma}^{M_{X_k}}(q^2) =& \frac{\mathrm{i}}{2}\int \mathrm{d}^4x\mathrm{e}^{\mathrm{i}q\cdot x}\langle 0|T(j_{\mu\nu}^{X_A}(x)j_\sigma^{X_{B_k}+}(0)\\ &+ j_\sigma^{X_{B_k}}(x)j_{\mu\nu}^{X_A+}(0))|0\rangle\\ \sim& \left(\frac{\lambda_{X_A}}{M_H}\epsilon_{\mu\nu\alpha\beta}\varepsilon_\alpha^{X_A}q_\beta\right)(\lambda_{X_{B_k}}^*\varepsilon_\sigma^{*X_{B_k}})\\ &+\left(\frac{\lambda_{X_A}^*}{M_H}\epsilon_{\mu\nu\alpha\beta}\varepsilon_\alpha^{*X_A}q_\beta\right)(\lambda_{X_{B_k}}\varepsilon_\sigma^{X_{B_k}})+\ldots\\ =& \frac{\lambda_{X_A}\lambda_{X_{B_k}}^*+\lambda_{X_A}^*\lambda_{X_{B_k}}}{M_H}q_\alpha\epsilon_{\mu\nu\sigma\alpha}+\ldots,\end{aligned} \tag{22}$$

where $k=1,2;\varepsilon_{\alpha/\sigma}^{X_A/X_{B_k}}$ is a polarization vector; M_H represents the ground state mass of X_A; and dots represent excited contributions to the spectral density and polynomial subtraction terms. In the definition of the mixing strength Eq. (14), we have omitted the Lorentz structures of corresponding currents. The dimension of the decay constant depends on the Lorentz structure we extract in the diagonal correlator. If the two currents have different Lorentz structures, we need to compensate the mass dimension of the decay constants, which are obtained from previous works, to make the mixing strength Eq. (14) dimensionless. The normal method is to make the Lorentz structures massless by multipling a factor M_H^n with a suitable n. Hence, we define λ_{X_A}/M_H as the new coupling constant of the X_A state. The mixing strength can be written as

$$\begin{aligned}
N_{M_{X_1}} &= \frac{0.168\text{GeV}^9\times M_H(3.798\text{GeV})}{\sqrt{1.49}\text{GeV}^5\times\sqrt{2.24}\text{GeV}^5} = 0.349,\\
\widetilde{N}_{M_{X_1}} &= \sin^2\left(\frac{\arcsin(0.349\times 2)}{2}\right) = 14\%,\\
N_{M_{X_2}} &= \frac{0.760\text{GeV}^9\times M_H(3.798\text{GeV})}{\sqrt{1.49}\text{GeV}^5\times\sqrt{69.0}\text{GeV}^5} = 0.285,\\
\widetilde{N}_{M_{X_2}} &= \sin^2\left(\frac{\arcsin(0.285\times 2)}{2}\right) = 9.0\%,\\
N_{M_C} &= \frac{0.0282\text{GeV}^{10}}{\sqrt{0.0229}\text{GeV}^5\times\sqrt{2.24}\text{GeV}^5} = 0.125,\\
\widetilde{N}_{M_C} &= \sin^2\left(\frac{\arcsin(0.125\times 2)}{2}\right) = 1.6\%,
\end{aligned} \tag{23}$$

The state $M_{X_1}(3987)$ is a mixture of $X_A(3798)$ and $X_{B_1}(3857)$, which have similar mass predictions close to $X(3872)$; unsurprisingly, this state also has the same mass prediction. Due to $X(3872)$, observed decays to $\pi^+\pi^- J/\psi(1S)$, $\omega J/\psi(1S)$ and $\bar{D}^{*0}D^0$, $M_{X_1}(3987)$ is a good candidate to describe $X(3872)$ [2]. We can estimate the proportions of each constituent and decay width of the corresponding decay modes by using the parameter $N_{M_{X_1}}$. Experimental results of $X(3872)$ decay width Γ_1 of the $\bar{Q}q+Q\bar{q}$ like decay mode is >30%, while the decay width Γ_2 of the $\bar{Q}Q+\bar{q}q$ like decay mode is >5%. By comparison, the parameter $N_{M_{X_1}}$ shows that the proportions of the $\bar{Q}qQ\bar{q}$ and $\bar{Q}Q\bar{q}q$ parts of $M_{X_1}(3987)$ are 86% and 14%, respectively. Considering the similar Lorentz-invariant phase-space of these two kinds of decay modes, we can roughly equate Γ_1/Γ_2 to the ratio of these two parts, 86%/14% ~ 6, which is consistent with experimental results. It should be noted that our method can not determine definitely which constitute dominates the mixing state. We tend to the one whose pure mass is closer to the mixing state.

When we consider the two-quark state $j_\mu^{X_C}$, the corresponding mixing angle is arcsin (0.25)/2 = 7°, which is consistent with the result in Ref. [28], and the dominant part of M_C is $j_\mu^{X_C}$. However, we found that this result strongly depends on the normalization of $j_\mu^{X_C}$. Hence, a proper normalized current is essential in calculations.

For the state $M_{X_2}(4945)$, its mass prediction is larger than those for all observed 1^{++} states. However, our calculation suggests that it is relatively strongly mixed. The dominant part of $M_{X_2}(4945)$ is more likely to be $X_{B_2}(5310)$ by comparing mass predictions.

In Ref. [19], the authors calculated the state X_{B_1} with a similar method and obtained the following results: the mass $m_{X_{B_1}} = 3.89^{+0.09}_{-0.09}$ GeV and the decay constant $\lambda_{X_{B_1}} = 2.96^{+1.09}_{-0.79}\times 10^{-4}$ GeV^{10} with $\sqrt{s_0} = 4.41$ GeV, which is consistent with our results.

IV. MIXED STATE IN 1^{--} CHANNEL

We start from two forms of currents as follows:

$$\begin{aligned}
j_\mu^{Y_{A_1}/Y_{A_{s1}}}(x) &= \bar{c}(x)c(x)\bar{q}(x)\gamma_\mu q(x),\\
j_\mu^{Y_{A_2}/Y_{A_{s2}}}(x) &= \bar{c}(x)\gamma_\mu c(x)\bar{q}(x)q(x),\\
j_\mu^{Y_{B_1}/Y_{B_{s1}}}(x) &= \frac{\mathrm{i}}{\sqrt{2}}[\bar{c}(x)\gamma_\mu q(x)\bar{q}(x)c(x)\\
&\quad + \bar{q}(x)\gamma_\mu c(x)\bar{c}(x)q(x)],\\
j_\mu^{Y_{B_2}/Y_{B_{s2}}}(x) &= \frac{\mathrm{i}}{\sqrt{2}}[\bar{c}(x)\gamma_\mu\gamma_5 q(x)\bar{q}(x)\gamma_5 c(x)\\
&\quad - \bar{q}(x)\gamma_\mu\gamma_5 c(x)\bar{c}(x)\gamma_5 q(x)],
\end{aligned} \tag{24}$$

where Y denotes the 1^{--} state; the subscript A of Y represents the $\bar{Q}Q\bar{q}q$ scenario, while B represents the $\bar{Q}qQ\bar{q}$ scenario. The additional subscript s represents the s quark case, and one can straightforwardly replace the q with the s quark when $j_\mu^{Y_{A_{s1}}}$, $j_\mu^{Y_{A_{s2}}}$, $j_\mu^{Y_{B_{s1}}}$, and $j_\mu^{Y_{B_{s2}}}$ are involved. The $Y(4230)$ was observed to decay to $\chi_{c0}\omega$, while $Y(4660)$ was observed to have both the $\psi(2S)\pi^+\pi^-$ and $D_s^+D_{s1}(2536)^-$ decay modes [2]. Hence, we especially focus on the currents $j_\mu^{Y_{A_1}}$ and $j_\mu^{Y_{A_{s2}}}$, which are consistent with the respective decay modes, to describe $Y(4230)$ and $Y(4660)$, respectively, and discuss the corresponding mixed states in both the u,d and s quarks for simplicity.

The two-point correlator functions of the pure states have the Lorentz structures

$$\begin{aligned}
\Pi_{\mu\nu}^{Y_{A_k}/Y_{A_{sk}}}(q^2) &= \Pi_{(1)}^{Y_{A_k}/Y_{A_{sk}}}(q^2)\left(-g_{\mu\nu}+\frac{q_\mu q_\nu}{q^2}\right)\\
&\quad + \Pi_{(0)}^{Y_{A_k}/Y_{A_{sk}}}(q^2)\left(\frac{q_\mu q_\nu}{q^2}\right),\\
\Pi_{\mu\nu}^{Y_{B_k}/Y_{B_{sk}}}(q^2) &= \Pi_{(1)}^{Y_{B_k}/Y_{B_{sk}}}(q^2)\left(-g_{\mu\nu}+\frac{q_\mu q_\nu}{q^2}\right)\\
&\quad + \Pi_{(0)}^{Y_{B_k}/Y_{B_{sk}}}(q^2)\left(\frac{q_\mu q_\nu}{q^2}\right),
\end{aligned} \tag{25}$$

where $k=1,2;\Pi_{(1)}^{Y_{A_k}/Y_{A_{sk}}}$ and $\Pi_{(1)}^{Y_{B_k}/Y_{B_{sk}}}$ describe pure state contributions with quantum numbers 1^{--}; and $\Pi_{(0)}^{Y_{A_k}/Y_{A_{sk}}}$ and $\Pi_{(0)}^{Y_{B_k}/Y_{B_{sk}}}$ describe the pure state contribution with quantum numbers 0^{+-}.

To study the mixed state, the off-diagonal mixing two-point correlation functions described in Section II are

$$\begin{aligned}
\Pi_{\mu\nu}^{M_{Y_1}}(q^2)=&\frac{\mathrm{i}}{2}\int \mathrm{d}^4x\mathrm{e}^{\mathrm{i}q\cdot x}\langle 0|T(j_\mu^{Y_{A_1}}(x)j_\nu^{Y_{B_1}+}(0)\\
&+j_\nu^{Y_{B_1}}(x)j_\mu^{Y_{A_1}+}(0))|0\rangle,\\
\Pi_{\mu\nu}^{M_{Y_2}}(q^2)=&\frac{\mathrm{i}}{2}\int \mathrm{d}^4x\mathrm{e}^{\mathrm{i}q\cdot x}\langle 0|T(j_\mu^{Y_{A_1}}(x)j_\nu^{Y_{B_2}+}(0)\\
&+j_\nu^{Y_{B_2}}(x)j_\mu^{Y_{A_1}+}(0))|0\rangle,\\
\Pi_{\mu\nu}^{M_{Y_{s1}}}(q^2)=&\frac{\mathrm{i}}{2}\int \mathrm{d}^4x\mathrm{e}^{\mathrm{i}q\cdot x}\langle 0|T(j_\mu^{Y_{A_{s2}}}(x)j_\nu^{Y_{B_{s1}}+}(0)\\
&+j_\nu^{Y_{B_{s1}}}(x)j_\mu^{Y_{A_{s2}}+}(0))|0\rangle,\\
\Pi_{\mu\nu}^{M_{Y_{s2}}}(q^2)=&\frac{\mathrm{i}}{2}\int \mathrm{d}^4x\mathrm{e}^{\mathrm{i}q\cdot x}\langle 0|T(j_\mu^{Y_{A_{s2}}}(x)j_\nu^{Y_{B_{s2}}+}(0)\\
&+j_\nu^{Y_{B_{s2}}}(x)j_\mu^{Y_{A_{s2}}+}(0))|0\rangle,
\end{aligned}\tag{26}$$

where M_{Y_k} and $M_{Y_{sk}}$, with $k=1,2$, both represent mixed states coupled to their respective currents. These mixed correlators have the same Lorentz structures as the pure state cases,

$$\begin{aligned}
\Pi_{\mu\nu}^{M_{Y_k}/M_{Y_{sk}}}(q^2)=&\Pi_{(1)}^{M_{Y_k}/M_{Y_{sk}}}(q^2)\left(-g_{\mu\nu}+\frac{q_\mu q_\nu}{q^2}\right)\\
&+\Pi_{(0)}^{M_{Y_k}/M_{Y_{sk}}}(q^2)\left(\frac{q_\mu q_\nu}{q^2}\right),
\end{aligned}\tag{27}$$

where $k=1,2$, and $\Pi_{(1)}^{M_{Y_k}/M_{Y_{sk}}}$ and $\Pi_{(0)}^{M_{Y_k}/M_{Y_{sk}}}$ describe the mixed states with quantum numbers 1^{--} and 0^{+-}, respectively.

We follow same method mentioned in the 1^{++} channel. The mesonic structures, mass and coupling constant predictions, and the related QCDSR parameters are presented in Table 4.

In the Y family of states, $Y(4160)$, $Y(4260)$, $Y(4415)$, $Y(4660)$ are reported to have decay modes including an s quark in the final states, and $Y(4230)$, $Y(4360)$, and $Y(4390)$ have not been observed to have decay modes that include an s quark in the final states. Furthermore, $Y(4260)$ only decays to the K meson while $Y(4415)$ and $Y(4660)$ only decay to the D_s meson when an s quark is directly involved in the final states. The $Y(4160)$ has both decay modes, including the K and D_s mesons in the final states. In contrast, all Y states have both $\bar{Q}Q+\bar{q}q$ like decay modes and $\bar{Q}q+Q\bar{q}$ like decay modes, with the exception of $Y(4390)$. The decay mode $Y(4390)$ to $\pi^+\pi^-h_c$ was observed, but the other decay modes of $Y(4390)$ have not yet been seen. We cannot exclude an s quark in $Y(4230)$, $Y(4360)$, $Y(4390)$ because the K meson may decay to the π meson and disappear in the final states [2]. Hence, we suggest that $Y(4230)$ has candidates $Y_{A_1}(4207)$, $M_{Y_2}(4266)$, and $Y(4360)$; $Y(4390)$ has a candidate $Y_{B_2}(4385)$; $Y(4415)$ has candidates $Y_{B_{s2}}(4494)$ and $M_{Y_{s2}}(4450)$; and $Y(4660)$ has candidates $Y_{A_{s2}}(4621)$ and $M_{Y_{s1}}(4610)$. Although the remaining states are not compatible with known 1^{--} states, they still possibly mix with other states, and their contributions can be estimated.

For the 1^{--} states, the mixing strengths are given by the data in Table 4:

$$\begin{aligned}
N_{M_{Y_1}}&=\frac{1.16\mathrm{GeV}^{10}}{\sqrt{1.64}\mathrm{GeV}^5\times\sqrt{34.5}\mathrm{GeV}^5}=0.15,\\
N_{M_{Y_2}}&=\frac{0.373\mathrm{GeV}^{10}}{\sqrt{1.64}\mathrm{GeV}^5\times\sqrt{7.36}\mathrm{GeV}^5}=0.11,\\
N_{M_{Y_{s1}}}&=\frac{2.56\mathrm{GeV}^{10}}{\sqrt{21.3}\mathrm{GeV}^5\times\sqrt{37.9}\mathrm{GeV}^5}=0.09,\\
N_{M_{Y_{s2}}}&=\frac{1.64\mathrm{GeV}^{10}}{\sqrt{21.3}\mathrm{GeV}^5\times\sqrt{9.60}\mathrm{GeV}^5}=0.11.
\end{aligned}\tag{28}$$

All mixed states have a much weaker mixing strength compared with the 1^{++} mixed states. We suggest that 1^{--} states are preferred to be pure and weakly mixed with other states. This becomes more clear when we convert N to $\widetilde{N}$,

$$\begin{aligned}
\widetilde{N}_{M_{Y_1}}&=\sin^2\left(\frac{\arcsin(0.15\times2)}{2}\right)=2.3\%,\\
\widetilde{N}_{M_{Y_2}}&=\sin^2\left(\frac{\arcsin(0.11\times2)}{2}\right)=1.2\%,\\
\widetilde{N}_{M_{Y_{s1}}}&=\sin^2\left(\frac{\arcsin(0.09\times2)}{2}\right)=0.82\%,\\
\widetilde{N}_{M_{Y_{s2}}}&=\sin^2\left(\frac{\arcsin(0.11\times2)}{2}\right)=1.2\%,
\end{aligned}\tag{29}$$

where the values of $\widetilde{N}$ suggest that the assumed mixed states with quantum numbers 1^{--} are actually very pure. As mentioned above, $M_{Y_1}(4770)$, which contains no s quark, is close to $Y(4660)$ and cannot be compatible with known 1^{--} states. $M_{Y_2}(4266)$, which is a possible candidate for $Y(4230)$, is a mixture of $Y_{A_1}(4207)$ and $Y_{B_2}(4385)$. By comparing the two mass predictions, $M_{Y_2}(4266)$ is closer to $Y_{A_1}(4207)$ rather than $Y_{B_2}(4385)$, and it is possibly dominated by $\bar{Q}Q\bar{q}q$ component. For the same reasons, $M_{Y_{s1}}(4610)$ is possibly dominated by a $\bar{Q}Q\bar{q}q$ component, while $M_{Y_{s2}}(4450)$ is possibly dominated by $\bar{Q}q\bar{Q}q$. Hence, we suggest that $Y(4230)$ and $Y(4660)$ prefer a $\bar{Q}Q\bar{q}q$ state, and $Y(4415)$ prefers a $\bar{Q}q\bar{Q}q$ state.

In Ref. [30], authors have calculated the states Y_{B_1} and Y_{B_2} with a similar method and obtained the follow-

Table 4. Summary of results for 1^{--} states.

State	Current structure	Mass/GeV	$\lambda/10^{-4}\,\mathrm{GeV}^{10}$	$\sqrt{s_0}$/GeV	τ window/GeV^{-2}
Y_{A_1}	$\chi_{c0}\omega$	$4.207^{+0.08}_{-0.09}$	$1.64^{+0.63}_{-0.49}$	4.8	0.27 – 0.28
$Y_{A_{s2}}$	$J/\psi f(980)$	$4.621^{+0.05}_{-0.06}$	$21.3^{+5.2}_{-4.7}$	5.1	0.25 – 0.32
Y_{B_1}	$D_0^*\bar{D}^*$	$4.922^{+0.04}_{-0.04}$	$34.5^{+6.7}_{-6.0}$	5.4	0.21 – 0.34
Y_{B_2}	$D_1\bar{D}$	$4.385^{+0.06}_{-0.06}$	$7.36^{+1.95}_{-1.67}$	4.9	0.27 – 0.35
$Y_{B_{s1}}$	$D_{s0}^*\bar{D}_s^*$	$4.952^{+0.03}_{-0.04}$	$37.9^{+6.5}_{-6.3}$	5.45	0.21 – 0.36
$Y_{B_{s2}}$	$D_{s1}\bar{D}_s$	$4.494^{+0.08}_{-0.05}$	$9.60^{+3.7}_{-2.1}$	5.0	0.26 – 0.39
M_{Y_1}	$\chi_{c0}\omega$ - $D_0^*\bar{D}^*$	$4.770^{+0.07}_{-0.06}$	$1.16^{+0.37}_{-0.28}$	5.3	0.24 – 0.25
M_{Y_2}	$\chi_{c0}\omega$ - $D_1\bar{D}$	$4.266^{+0.08}_{-0.08}$	$0.373^{+0.117}_{-0.093}$	4.95	0.26 – 0.27
$M_{Y_{s1}}$	$J/\psi f(980)$ - $D_{s0}^*\bar{D}_s^*$	$4.610^{+0.05}_{-0.06}$	$2.56^{+0.67}_{-0.56}$	5.1	0.24 – 0.33
$M_{Y_{s2}}$	$J/\psi f(980)$ - $D_{s1}\bar{D}_s$	$4.450^{+0.05}_{-0.06}$	$1.64^{+0.43}_{-0.22}$	4.95	0.26 – 0.33

ing results: mass $m_{Y_{B_1}} = 4.78^{+0.07}_{-0.07}$ with $\sqrt{s_0} = 5.3$ GeV^{-2}, and mass $m_{Y_{B_2}} = 4.36^{+0.08}_{-0.08}$ with $\sqrt{s_0} = 4.9$ GeV^{-2}; these numbers are consistent with our results. The small difference in the mass of Y_{B_1} is caused by the different values of $\sqrt{s_0}$. In addition, in Ref. [30], the authors have discussed different results of the similar states of Y_{B_1} and Y_{B_2} in previous papers. For instance, the authors in Ref. [42] did not distinguish between the charge conjugations and obtained mass of a Y_{B_1} like state $m_{D_0^*\bar{D}^*} = 4.26$ GeV. Our results are more supportive of the results in Ref. [30].

In Ref. [8], the authors have calculated the states $Y_{A_{s2}}$ with a similar method and obtained the following result: mass $m_{Y_{A_{s2}}} = 4.67^{+0.09}_{-0.09}$ with $\sqrt{s_0} = 5.1$ GeV^{-2}; this is consistent with our result.

V. MIXED STATE IN 1^{-+} CHANNEL

We start from two forms of currents as follows:

$$\begin{aligned}
j_{\mu\nu}^{P_A}(x) &= j_{\mu\nu}^{X_A}(x),\\
j_{\mu\nu}^{P_{A_s}}(x) &= \frac{\mathrm{i}}{\sqrt{2}}[\bar{c}(x)\gamma_\mu c(x)\bar{s}(x)\gamma_\nu s(x)\\
&\quad - \bar{c}(x)\gamma_\nu c(x)\bar{s}(x)\gamma_\mu s(x)],\\
j_{\mu}^{P_{B_1}/P_{B_{s1}}}(x) &= \frac{\mathrm{i}}{\sqrt{2}}[\bar{c}(x)\gamma_\mu q(x)\bar{q}(x)c(x)\\
&\quad - \bar{q}(x)\gamma_\mu c(x)\bar{c}(x)q(x)],\\
j_{\mu}^{P_{B_2}/P_{B_{s2}}}(x) &= \frac{\mathrm{i}}{\sqrt{2}}[\bar{c}(x)\gamma_\mu\gamma_5 q(x)\bar{q}(x)\gamma_5 c(x)\\
&\quad + \bar{q}(x)\gamma_\mu\gamma_5 c(x)\bar{c}(x)\gamma_5 q(x)],
\end{aligned} \tag{30}$$

where P denotes the 1^{-+} state; the subscript A of P represents the $\bar{Q}Q\bar{q}q$ scenario, while B represents the $\bar{Q}q\bar{Q}q$ scenario. The additional subscript s represents the s quark case, and one can straightforwardly replace q with s when $j_\mu^{P_{B_{s1}}}$ and $j_\mu^{P_{B_{s2}}}$ are involved. The structures of these currents are similar to the 1^{++} and 1^{--} cases, and it is interesting to compare the mass predictions of these currents to the 1^{++} and 1^{--} states.

To study the pure $\bar{Q}Q\bar{q}q$ and $\bar{Q}q\bar{Q}q$ states, the two-point correlation functions have the respective Lorentz structures,

$$\begin{aligned}
\Pi_{\mu\nu\rho\sigma}^{P_A/P_{A_s}}(q^2) =& \Pi_a^{P_A/P_{A_s}}\frac{1}{q^2}(q^2 g_{\mu\rho}g_{\nu\sigma} - q^2 g_{\mu\sigma}g_{\nu\rho}\\
&- q_\mu q_\rho g_{\nu\sigma} + q_\mu q_\sigma g_{\nu\rho} - q_\nu q_\sigma g_{\mu\rho} + q_\nu q_\rho g_{\mu\sigma})\\
&+ \Pi_b^{P_A/P_{A_s}}\frac{1}{q^2}(-q_\mu q_\rho g_{\nu\sigma} + q_\mu q_\sigma g_{\nu\rho}\\
&- q_\nu q_\sigma g_{\mu\rho} + q_\nu q_\rho g_{\mu\sigma}),\\
\Pi_{\mu\nu}^{P_{B_k}/P_{B_{sk}}}(q^2) =& \Pi_{(1)}^{P_{B_k}/P_{B_{sk}}}(q^2)\left(-g_{\mu\nu} + \frac{q_\mu q_\nu}{q^2}\right)\\
&+ \Pi_{(0)}^{P_{B_k}/P_{B_{sk}}}(q^2)\left(\frac{q_\mu q_\nu}{q^2}\right),
\end{aligned} \tag{31}$$

where $k = 1, 2$; $\Pi_a^{P_A/P_{A_s}}$ and $\Pi_b^{P_A/P_{A_s}}$ describe the pure state contributions with quantum numbers 1^{++} and 1^{-+}, respectively; and $\Pi_{(1)}^{P_{B_k}/P_{B_{sk}}}$ and $\Pi_{(0)}^{P_{B_k}/P_{B_{sk}}}$ describe 1^{-+} and 0^{++}, respectively. In mixing scenarios, we start from the off-diagonal mixed correlator described in the previous sections, i.e.,

$$\begin{aligned}
\Pi_{\mu\nu\sigma}^{M_{P_1}/M_{P_{s1}}}(q^2) =& \frac{\mathrm{i}}{2}\int \mathrm{d}^4x\, \mathrm{e}^{\mathrm{i}q\cdot x}\langle 0|T(j_{\mu\nu}^{P_A/P_{A_s}}(x) j_\sigma^{P_{B_1}/P_{B_{s1}}+}(0)\\
&+ j_\sigma^{P_{B_1}/P_{B_{s1}}}(x) j_{\mu\nu}^{P_A/P_{A_s}+}(0))|0\rangle,\\
\Pi_{\mu\nu\sigma}^{M_{P_2}/M_{P_{s2}}}(q^2) =& \frac{\mathrm{i}}{2}\int \mathrm{d}^4x\, \mathrm{e}^{\mathrm{i}q\cdot x}\langle 0|T(j_{\mu\nu}^{P_A/P_{A_s}}(x) j_\sigma^{P_{B_2}/P_{B_{s2}}+}(0)\\
&+ j_\sigma^{P_{B_2}/P_{B_{s2}}}(x) j_{\mu\nu}^{P_A/P_{A_s}+}(0))|0\rangle,
\end{aligned} \tag{32}$$

where $M_{P_k}/M_{P_{sk}}$, with $k = 1, 2$, are mixed states assumed to result from the corresponding currents. The correlators

have the Lorentz structure

$$\Pi^{M_{P_k}/M_{P_{sk}}}_{\mu\nu\sigma}(q^2)=\Pi^{M_{P_k}/M_{P_{sk}}}(q^2)(-g_{\mu\sigma}q_\nu+g_{\nu\sigma}q_\mu). \tag{33}$$

We follow same method used in previous sections. The mesonic structures, mass and coupling constant predictions, and related QCDSR parameters are presented in Table 5.

All pure states have mass predictions of over 4.5 GeV and cannot be compatible with those known states, which are probably 1^{-+} candidates [2].

The mixing strength can then be estimated by computing the value of N. Note that the coupling constants of the mixed state correlator has the form

$$\begin{aligned}\Pi^{M_{P_k}}_{\mu\nu\sigma}(q^2)=&\frac{\mathrm{i}}{2}\int \mathrm{d}^4x\mathrm{e}^{\mathrm{i}q\cdot x}\langle 0|T(j^{P_A}_{\mu\nu}(x)j^{P_{B_k}+}_{\sigma}(0)\\&+j^{P_{B_k}}_{\sigma}(x)j^{P_A+}_{\mu\nu}(0))|0\rangle\\&\sim\frac{\lambda_{P_A}}{M_H}(\varepsilon^{P_A}_{\mu}q_\nu-\varepsilon^{P_A}_{\nu}q_\mu)(\lambda^*_{P_{B_k}}\varepsilon^{*P_{B_k}}_{\sigma})\\&+\frac{\lambda^*_{P_A}}{M_H}(\varepsilon^{*P_A}_{\mu}q_\nu-\varepsilon^{*P_A}_{\nu}q_\mu)(\lambda_{P_{B_k}}\varepsilon^{P_{B_k}}_{\sigma})+\ldots\\=&\frac{\lambda_{P_A}\lambda^*_{P_{B_k}}+\lambda^*_{P_A}\lambda_{P_{B_k}}}{M_H}(-g_{\mu\sigma}q_\nu+g_{\nu\sigma}q_\mu)+\ldots,\end{aligned} \tag{34}$$

where $k=1,2$; ε^{P_A} and $\varepsilon^{P_{B_k}}$ are polarization vectors; and M_H represents the ground state mass of P_A. Analogous to the 1^{++} channel, the values of N obtained from Table 5 can be written as

$$\begin{aligned}N_{M_{P_1}}=&\frac{0.401\mathrm{GeV}^9\times M_H(4.658\mathrm{GeV})}{\sqrt{13.1}\mathrm{GeV}^5\times\sqrt{34.1}\mathrm{GeV}^5}=0.09,\\N_{M_{P_2}}=&\frac{0.240\mathrm{GeV}^9\times M_H(4.658\mathrm{GeV})}{\sqrt{13.1}\mathrm{GeV}^5\times\sqrt{9.7}\mathrm{GeV}^5}=0.10,\end{aligned}$$

$$\begin{aligned}N_{M_{P_{s1}}}=&\frac{0.405\mathrm{GeV}^9\times M_H(4.694\mathrm{GeV})}{\sqrt{14.0}\mathrm{GeV}^5\times\sqrt{42.8}\mathrm{GeV}^5}=0.08,\\N_{M_{P_{s2}}}=&\frac{0.269\mathrm{GeV}^9\times M_H(4.694\mathrm{GeV})}{\sqrt{14.0}\mathrm{GeV}^5\times\sqrt{13.0}\mathrm{GeV}^5}=0.09,\end{aligned} \tag{35}$$

where M_H represents the corresponding $\bar{Q}Q\bar{q}q$ ground state mass. Like the 1^{--} channel, all the mixed states that have quantum numbers 1^{-+} are weakly mixed with corresponding currents; this becomes clearer when we convert N to $\widetilde{N}$,

$$\begin{aligned}\widetilde{N}_{M_{P_1}}=&\sin^2\left(\frac{\arcsin(0.09\times2)}{2}\right)=0.82\%,\\\widetilde{N}_{M_{P_2}}=&\sin^2\left(\frac{\arcsin(0.10\times2)}{2}\right)=1.0\%,\\\widetilde{N}_{M_{P_{s1}}}=&\sin^2\left(\frac{\arcsin(0.08\times2)}{2}\right)=0.64\%,\\\widetilde{N}_{M_{P_{s2}}}=&\sin^2\left(\frac{\arcsin(0.09\times2)}{2}\right)=0.82\%.\end{aligned} \tag{36}$$

For the same reasons mentioned in the 1^{--} channel, $M_{P_1}(4505)$ and $M_{P_{s1}}(4494)$ are dominated by the $\bar{Q}Q\bar{q}q$ components; $M_{P_2}(4544)$ and $M_{P_{s2}}(4536)$ are more likely dominated by the $\bar{Q}q\bar{Q}\bar{q}$ components.

In Ref. [30], authors have calculated the states P_{B_1} and P_{B_2} with a similar method and obtained the following results: mass $m_{P_{B_1}}=4.73^{+0.07}_{-0.07}$ with $\sqrt{s_0}=5.2$ GeV^{-2}, and mass $m_{P_{B_2}}=4.60^{+0.08}_{-0.08}$ with $\sqrt{s_0}=5.1$ GeV^{-2}; these numbers are consistent with our results. The small difference in the mass of P_{B_1} is caused by the different values of $\sqrt{s_0}$. Moreover, the authors in Ref. [43] obtained the mass of state P_{B_1}, $m_{P_{B_1}}=4.19$ GeV. Our results are more supportive of the results in Ref. [30].

Table 5. Summary of results for 1^{-+} molecular states.

State	Current structure	Mass/GeV	$\lambda/10^{-4}\mathrm{GeV}^{10}$	$\sqrt{s_0}$/GeV	τ window/GeV^{-2}
P_A	$J/\psi\rho$	$4.658^{+0.05}_{-0.06}$	$13.1^{+3.2}_{-3.1}$	5.15	0.24 – 0.29
P_{A_s}	$J/\psi f(980)$	$4.694^{+0.05}_{-0.05}$	$14.0^{+3.5}_{-2.9}$	5.2	0.24 – 0.32
P_{B_1}	$D^*_0\bar{D}^*$	$4.927^{+0.05}_{-0.04}$	$34.1^{+7.7}_{-5.7}$	5.4	0.21 – 0.30
P_{B_2}	$D_1\bar{D}$	$4.528^{+0.06}_{-0.05}$	$9.7^{+2.9}_{-2.1}$	5.05	0.26 – 0.31
$P_{B_{s1}}$	$D^*_{s0}\bar{D}^*_s$	$4.999^{+0.04}_{-0.03}$	$42.8^{+8.2}_{-6.8}$	5.5	0.21 – 0.33
$P_{B_{s2}}$	$D_{s1}\bar{D}_s$	$4.642^{+0.05}_{-0.05}$	$13.0^{+3.4}_{-2.8}$	5.15	0.25 – 0.34
M_{P_1}	$J/\psi\rho$ - $D^*_0\bar{D}^*$	$4.505^{+0.06}_{-0.04}$	$0.401^{+0.096}_{-0.073}$ GeV^{-1}	5.05	0.21 – 0.30
M_{P_2}	$J/\psi\rho$ - $D_1\bar{D}$	$4.494^{+0.06}_{-0.06}$	$0.240^{+0.060}_{-0.052}$ GeV^{-1}	5.05	0.23 – 0.27
$M_{P_{s1}}$	$J/\psi f(980)$ - $D^*_{s0}\bar{D}^*_s$	$4.544^{+0.05}_{-0.05}$	$0.405^{+0.085}_{-0.077}$ GeV^{-1}	5.1	0.21 – 0.33
$M_{P_{s2}}$	$J/\psi f(980)$ - $D_{s1}\bar{D}_s$	$4.536^{+0.06}_{-0.05}$	$0.269^{+0.067}_{-0.055}$ GeV^{-1}	5.1	0.22 – 0.31

VI. NON-PERTURBATIVE EFFECTS OF MIXING STRENGTH

We can convert the $\bar{Q}Q\bar{q}q$ and $\bar{Q}qQ\bar{q}$ states to each other through the Fierz transformation. Generally,

$$\begin{aligned}(\bar{Q}\Gamma_1 Q)(\bar{q}\Gamma_2 q) &= \sum_{ijk} C_i(\bar{Q}\Gamma_j q)(\bar{q}\Gamma_k Q) \\ &+ \sum_{lmn} C_l(\bar{Q}\Gamma_m\lambda^a q)(\bar{q}\Gamma_n\lambda^a Q), \\ (\bar{Q}\Gamma_1 q)(\bar{q}\Gamma_2 Q) &= \sum_{ijk} C_i(\bar{Q}\Gamma_j Q)(\bar{q}\Gamma_k q) \\ &+ \sum_{lmn} C_l(\bar{Q}\Gamma_m\lambda^a Q)(\bar{q}\Gamma_n\lambda^a q),\end{aligned} \tag{37}$$

where Γ_i are gamma matrices, C_i are the parameters corresponding to the related currents, and λ^a are Gell-Mann matrices. That is, $\bar{Q}Q\bar{q}q$ currents can be decomposed into a series of $\bar{Q}qQ\bar{q}$ currents and a series of $\bar{Q}qQ\bar{q}$ color-octet currents, and vice versa. In this study, we have computed two-point correlation functions of $\bar{Q}Q\bar{q}q$ and $\bar{Q}qQ\bar{q}$ currents. One can convert one current to a series of other kinds of currents and make calculations analogous to a series of calculations of pure currents. For instance,

$$\begin{aligned}j_\mu^{Y_{A_1}} &= (\bar{c}c)(\bar{q}\gamma_\mu q) \\ &= \frac{-\mathrm{i}}{2\sqrt{2}}\frac{\mathrm{i}}{\sqrt{2}}[(\bar{c}\gamma_\mu q)(\bar{q}c) + (\bar{q}\gamma_\mu c)(\bar{c}q)] \\ &+ \frac{-\mathrm{i}}{2\sqrt{2}}\frac{\mathrm{i}}{\sqrt{2}}[(\bar{c}\gamma_\mu\gamma_5 q)(\bar{q}\gamma_5 c) - (\bar{q}\gamma_\mu\gamma_5 c)(\bar{c}\gamma_5 q)] \\ &+ \ldots \\ &= \frac{-\mathrm{i}}{2\sqrt{2}} j_\mu^{Y_{B_1}} + \frac{-\mathrm{i}}{2\sqrt{2}} j_\mu^{Y_{B_2}} + \ldots,\end{aligned} \tag{38}$$

where $j_\mu^{Y_{A_1}}$ and $j_\mu^{Y_{B_1/B_2}}$ are defined in Section IV. When we compute two-point correlation functions of $j_\mu^{Y_{A_1}}$ and $j_\mu^{Y_{B_1/B_2}}$, it seems that the result may highlight states Y_{B_1}/Y_{B_2}, and the parameters of the current decomposition are likely to be directly related to mixing strength. However, our calculations show different results. Although the contributions in perturbative terms from different currents (e.g., Y_{B_1} and Y_{B_2}) will be suppressed, QCDSR calculations are sensitive to the changes of borel window and threshold s_0, which depend on the contributions of non-perturbative terms. Moreover, the mixing strength is related to both decay constants and parameters of the corresponding currents from the Fierz transformation, and the decay constants are also sensitive to the Borel window, which again depends on non-perturbative terms. To clarify this, we have computed another two $\bar{Q}Q\bar{q}q$ and $\bar{Q}qQ\bar{q}$ currents and their mixed state,

$$\begin{aligned}j_\mu^{Z_A}(x) &= \bar{c}(x)\gamma_\mu c(x)\bar{q}(x)\gamma_5 q(x) \\ j_{\mu\nu}^{Z_B}(x) &= \frac{\mathrm{i}}{\sqrt{2}}[\bar{c}(x)\gamma_\mu q(x)\bar{q}(x)\gamma_\nu c(x) \\ &- \bar{q}(x)\gamma_\mu c(x)\bar{c}(x)\gamma_\nu q(x)],\end{aligned} \tag{39}$$

where Z denotes the 1^{+-} state, and the subscript A of Z represents the $\bar{Q}Q\bar{q}q$ scenario, while B represents the $\bar{Q}qQ\bar{q}$ scenario. The mixed state is described by

$$\begin{aligned}\Pi_{\mu\nu\sigma}^{M_Z}(q^2) = \frac{\mathrm{i}}{2}\int \mathrm{d}^4x\, \mathrm{e}^{\mathrm{i}q\cdot x}\langle 0|T(j_\sigma^{Z_A}(x) j_{\mu\nu}^{Z_B+}(0) \\ + j_{\mu\nu}^{Z_B}(x) j_\sigma^{P_A+}(0))|0\rangle,\end{aligned} \tag{40}$$

where M_Z is assumed to be mixed from corresponding currents. The hadronic structures along with results of mass, coupling constant, and mixing strength predictions are presented in Table 6.

Compared to the 1^{++} currents $j_\mu^{X_{A/B_1}}$ and their mixed two-point correlator $\Pi_{\mu\nu\sigma}^{M_{X_1}}(q^2)$, which are given in Eq. (17) and Eq. (19), $j_\mu^{Z_{A/B}}$ and $\Pi_{\mu\nu\sigma}^{M_Z}(q^2)$ have similar structures. According to our previous calculations in Section II, M_{X_1} is relatively strongly mixed with different components, and M_Z is supposed to have similar properties. However, the resulting mixing strength of M_Z is

$$\begin{aligned}N_{M_Z} &= \frac{0.054\mathrm{GeV}^9 \times M_H(4.018\mathrm{GeV})}{\sqrt{1.04}\mathrm{GeV}^5 \times \sqrt{2.90}\mathrm{GeV}^5} = 0.125, \\ \widetilde{N}_{M_Z} &= \sin^2\left(\frac{\arcsin(0.125\times 2)}{2}\right) = 1.6\%.\end{aligned} \tag{41}$$

Compared to M_{X_1} ($N_{M_{X_1}} = 0.349$, $\widetilde{N}_{M_{X_1}} = 14\%$), the mass predictions of two parts of the mixed state M_Z differ, and although the contributions of the perturbative terms in two-point correlator functions are similar, the mixing strength of the two states are quite different. Hence, we suggest that the mixing strength is consider-

Table 6. Summary of results for 1^{+-} states.

State	Current structure	Mass/GeV	$\lambda/10^{-4}\,\mathrm{GeV}^{10}$	$\sqrt{s_0}$/GeV	τ window/GeV^{-2}
Z_A	$J/\psi\eta$	$3.578^{+0.08}_{-0.08}$	$1.04^{+0.36}_{-0.27}$	4.2	0.33 – 0.34
Z_B	$D^*\bar{D}^*$	$4.018^{+0.06}_{-0.06}$	$2.90^{+0.88}_{-0.67}$	4.55	0.29 – 0.36
M_Z	$J/\psi\eta$ - $D^*\bar{D}^*$	$3.563^{+0.07}_{-0.06}$	$0.054^{+0.017}_{-0.012}$ GeV^{-1}	4.1	0.31 – 0.35

ably sensitive to the Borel window, threshold s_0, mass prediction, and decay constant, which are all influenced by non-perturbative terms in QCDSR calculations.

VII. SUMMARY

In this study, we used QCD sum-rules to calculate the mass spectrum of $\bar{Q}Q\bar{q}q$ and $\bar{Q}qQ\bar{q}$ states. Such states strongly couple to $\bar{Q}Q\bar{q}q$ or $\bar{Q}qQ\bar{q}$ currents. Therefore, state components of $\bar{Q}Q\bar{q}q$ and $\bar{Q}qQ\bar{q}$ can be mixed with each other. Such mixing can be studied via the mixed correlators of $\bar{Q}Q\bar{q}q$ and $\bar{Q}qQ\bar{q}$ currents. Our studies focus on the mixing strength, which may determine whether the mixing picture accommodates candidates that have more than single dominant decay modes.

We list all the mixed state results in Table 7. The uncertainties of the masses are less than 5%, and the uncertainties of the coupling constants are approximately 25%, which are induced by the uncertainties of the input parameters and threshold s_0. The relations $\sqrt{s_0} = M_H + \Delta_s$ and 40%–10% are required to determine the window of τ. These two conditions are not always satisfied well. In some cases, the windows of τ are very narrow. If higher dimension condensates are considered, we may reconsider the constraint of 40%–10%, and the situation may change.

For the 1^{++} channel, we find that the two states $M_{X_1}(3987)$ and $M_{X_2}(4945)$ are relatively strongly mixed with the $\bar{Q}Q\bar{q}q$ and $\bar{Q}qQ\bar{q}$ components. Furthermore, we estimate the ratio of decay width of two kinds of decay modes of $M_{X_1}(3987)$; this ratio is roughly consistent with the experimental results for $X(3872)$. When we consider the mixing state combined with $\bar{Q}Q$ and $\bar{Q}qQ\bar{q}$, we revisit the result in Ref. [28] with the new technique in Ref. [15]. The result argues that $\bar{Q}Q$ is the dominant part of $X(3872)$, which can explain the latest observation to $X(3872)$ of LHCb [7]. Our calculations just support that these two components can relatively strongly mix with each other in quantum numbers 1^{++}.

In other quantum number channels, states are found to be weakly mixed. However, the calculations of these states is still meaningful to help us establish the physical structure of a corresponding state. For instance, pure $\bar{Q}Q\bar{q}q$ $Y_{A_1}(4207)$ and $Y_{A_{s2}}(4610)$ configurations are good candidates for $Y(4230)$ and $Y(4660)$, respectively. However, by checking the assumed mixed states that mix with $\bar{Q}Q\bar{q}q$ and $\bar{Q}qQ\bar{q}$ molecular states, we find that these candidates have small components of $\bar{Q}qQ\bar{q}$; this is inconsistent with the fact that $Y(4230)$ and $Y(4660)$ have more abundant decay modes. Thus, we can establish the dominant part of $Y(4415)$. Our result suggests that $Y(4415)$ is dominated by $\bar{Q}qQ\bar{q}$ and agrees with the absence of the K meson in observed decay final states. However, $Y(4415)$ still has a small component of $\bar{Q}Q\bar{q}q$. These states may therefore have a more complicated construction; for instance, $\bar{q}q$ could be a color-octet state. Other models, such as the tetraquark model, could be valuable. By using the Fierz transformations, tetraquark currents can be decomposed into various molecular currents and color-octet currents, to show more mixed effects of different possible states [44]. Since the mixing effects are normally small, the studies via tetraquark currents cannot distinguish the details of mixing between the different currents and only give the average of those currents. As such, the tetraquark model is not a self-verifying because it cannot show which parts (via the Fierz transformations) interact with each other strongly and which ones do not. It may also address challenges in the quantitative descriptions of XYZ states.

The calculations based on pure molecular currents have been criticized because there is a large background of the two free mesons spectrum. If the states indeed have an absolutely dominate decay mode [45], there is no problem (actually, the mass of the molecule state is close

Table 7. Summary of mixed state results.

Mixed state	Mass/GeV	N	$\widetilde{N}$	Dominant part	Possible Candidate
M_{X_1}	$3.987^{+0.06}_{-0.06}$	0.349	14%	$\bar{Q}qQ\bar{q}$	$X(3872)$
M_{X_2}	$4.945^{+0.08}_{-0.06}$	0.285	9.0%	$\bar{Q}qQ\bar{q}$	–
M_C	$3.818^{+0.03}_{-0.02}$	0.125	1.6%	$\bar{Q}Q$	$X(3872)$
M_{Y_1}	$4.770^{+0.07}_{-0.06}$	0.15	2.3%	$\bar{Q}qQ\bar{q}$	–
M_{Y_2}	$4.266^{+0.08}_{-0.08}$	0.11	1.2%	$\bar{Q}Q\bar{q}q$	$Y(4230)$
$M_{Y_{s1}}$	$4.610^{+0.05}_{-0.06}$	0.06	<1%	$\bar{Q}Q\bar{q}q$	$Y(4660)$
$M_{Y_{s2}}$	$4.450^{+0.05}_{-0.06}$	0.11	1.2%	$\bar{Q}qQ\bar{q}$	$Y(4415)$
M_{P_1}	$4.505^{+0.06}_{-0.04}$	0.09	<1%	$\bar{Q}Q\bar{q}q$	–
M_{P_2}	$4.494^{+0.06}_{-0.06}$	0.10	1.0%	$\bar{Q}qQ\bar{q}$	–
$M_{P_{s1}}$	$4.544^{+0.05}_{-0.05}$	0.08	<1%	$\bar{Q}Q\bar{q}q$	–
$M_{P_{s2}}$	$4.536^{+0.06}_{-0.05}$	0.09	<1%	$\bar{Q}qQ\bar{q}$	–

to that of two free mesons). Otherwise, the mixing pattern must be taken into account. The mixing of the typical molecular currents $\bar{Q}Q\bar{q}q$ and $\bar{Q}q\bar{Q}\bar{q}$ are suppressed (perturbatively) by the small coefficients of Fierz transformations, so the background of the two free mesons spectrum is also suppressed. Non-perturbative corrections play more important roles in the mixing correlator, which can distinguish the real four-quark resonance from the two free mesons. It should be the essential feature of the mixing pattern. Our calculations show that the mixing pattern is consistent with some of the *XYZ* states but fails for many others. Since the mixing correlator is normalized by the two diagonal correlators, which may be affected by a large background of two free meson spectrum, the real mixture may be larger than our estimate. How to remove the background of the two free meson spectrum is still a major problem.

APPENDIX A: QCDSR ANALYSIS RESULTS

Here, we show the τ dependence of M_H^2 defined in Eq. (11) for all mixed states.

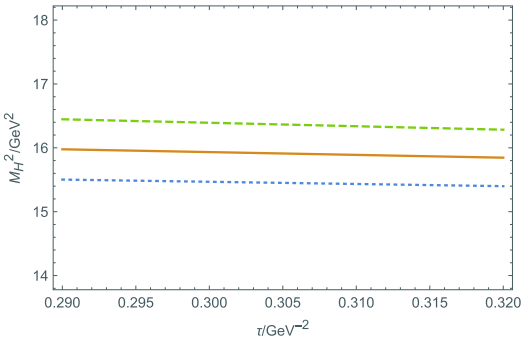

(a) M_H^2 dependence on τ for M_{X_1}. The solid line represents $\sqrt{s_0} = 4.4$GeV, and the dashed line and the dotted lines respectively represent $\sqrt{s_0} = 4.4 \pm 0.1$GeV .

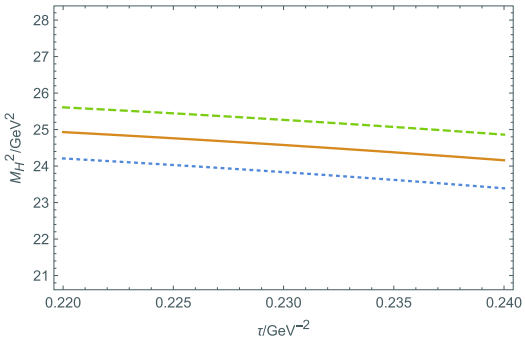

(b) M_H^2 dependence on τ for M_{X_2}. The solid line represents $\sqrt{s_0} = 5.45$GeV, and the dashed line and the dotted lines respectively represent $\sqrt{s_0} = 5.45 \pm 0.1$GeV.

Fig. A1. (color online) M_H^2 behaviors on τ for 1^{++} mixed states.

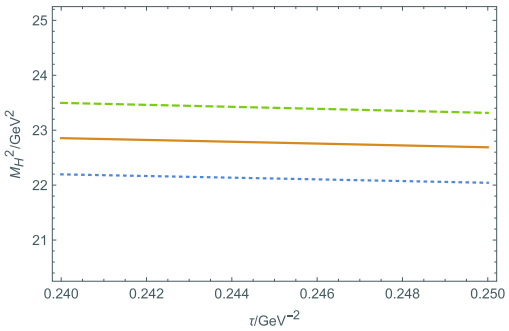

(a) M_H^2 dependence on τ for M_{Y_1}. The solid line represents $\sqrt{s_0} = 5.3$GeV, and the dashed line and the dotted line respectively represent $\sqrt{s_0} = 5.3 \pm 0.1$GeV.

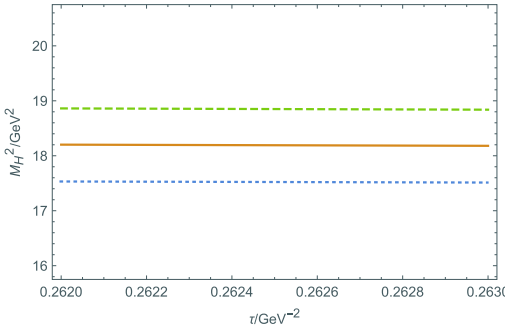

(b) M_H^2 dependence on τ for M_{Y_2}. The solid line represents $\sqrt{s_0} = 4.95$GeV, and the dashed line and the dotted line respectively represent $\sqrt{s_0} = 4.95 \pm 0.1$GeV.

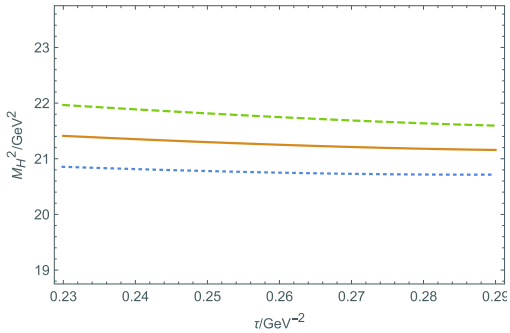

(c) M_H^2 dependence on τ for $M_{Y_{s1}}$. The solid line represents $\sqrt{s_0} = 5.1$GeV, and the dashed line and the dotted line respectively represent $\sqrt{s_0} = 5.1 \pm 0.1$GeV.

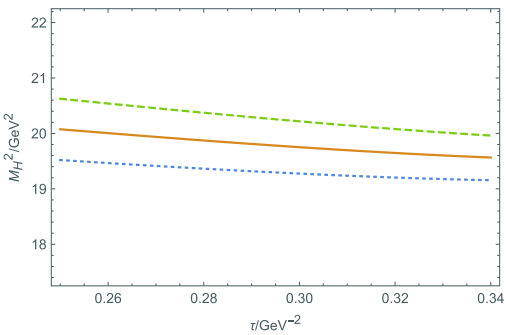

(d) M_H^2 dependence on τ for $M_{Y_{s2}}$. The solid line represents $\sqrt{s_0} = 4.95$GeV, and the dashed line and the dotted line respectively represent $\sqrt{s_0} = 4.95 \pm 0.1$GeV.

Fig. A2. (color online) M_H^2 behaviors on τ for 1^{--} mixed states.

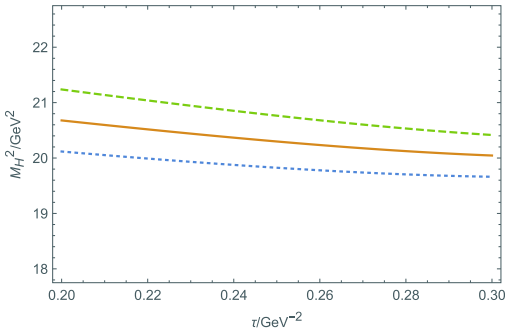

(a) M_H^2 dependence on τ for M_{P_1}. The solid line represents $\sqrt{s_0} = 5.05$GeV, and the dashed line and the dotted line respectively represent $\sqrt{s_0} = 5.05 \pm 0.1$GeV.

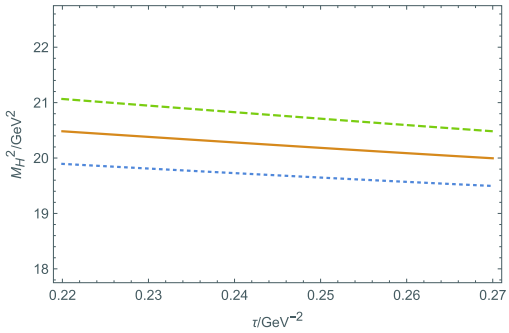

(b) M_H^2 dependence on τ for M_{P_2}. The solid line represents $\sqrt{s_0} = 5.05$GeV, and the dashed line and the dotted line respectively represent $\sqrt{s_0} = 5.05 \pm 0.1$GeV.

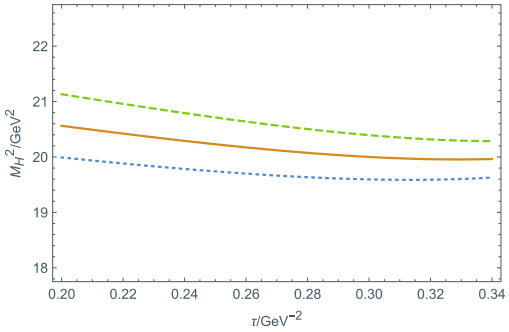

(c) M_H^2 dependence on τ for $M_{P_{s1}}$. The solid line represents $\sqrt{s_0} = 5.1$GeV, and the dashed line and the dotted line respectively represent $\sqrt{s_0} = 5.1 \pm 0.1$GeV.

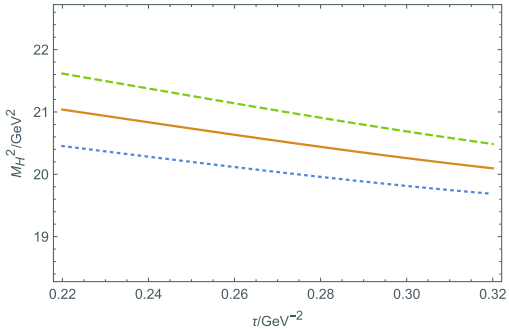

(d) M_H^2 dependence on τ for $M_{P_{s2}}$. The solid line represents $\sqrt{s_0} = 5.1$GeV, and the dashed line and the dotted line respectively represent $\sqrt{s_0} = 5.1 \pm 0.1$GeV.

Fig. A3. (color online) M_H^2 behaviors on τ for 1^{-+} mixed states.

References

[1] N. Brambilla, S. Eidelman, C. Hanhart *et al.*, Phys. Rept. **873**, 1 (2020), arXiv:10.1907.07583[hep-ex]

[2] P. A. Zyla *et al.* (Particle Data Group), PTEP **2020**, 083C01 (2020)

[3] R. M. Albuquerque, J. M. Dias, K. P. Khemchandani *et al.*, J. Phys. G **46**, 093002 (2019), arXiv:10.1812.08207[hep-ph]

[4] W. Chen and S.-L. Zhu, Phys. Rev. D **83**, 034010 (2011), arXiv:10.1010.3397[hep-ph]

[5] Q.-F. Lü and Y.-B. Dong, Phys. Rev. D **94**, 074007 (2016), arXiv:10.1607.05570[hep-ph]

[6] W. Chen, H.-y. Jin, R. T. Kleiv *et al.*, Phys. Rev. D **88**, 045027 (2013), arXiv:10.1305.0244[hep-ph]

[7] R. Aaij *et al.* (LHCb), Phys. Rev. Lett. **126**, 092001 (2021), arXiv:10.2009.06619[hep-ex]

[8] R. M. Albuquerque, M. Nielsen, and R. Rodrigues da Silva, Phys. Rev. D **84**, 116004 (2011), arXiv:10.1110.2113[hep-ph]

[9] S. I. Finazzo, M. Nielsen, and X. Liu, Phys. Lett. B **701**, 101 (2011), arXiv:10.1102.2347[hep-ph]

[10] F. E. Close and P. R. Page, Phys. Lett. B **366**, 323 (1996), arXiv:10. hep-ph/9507407

[11] M. Suzuki, Phys. Rev. D **72**, 114013 (2005), arXiv:10. hepph/0508258

[12] R. D. Matheus, S. Narison, M. Nielsen *et al.*, Phys. Rev. D **75**, 014005 (2007), arXiv:10. hep-ph/0608297

[13] C. E. Thomas and F. E. Close, Phys. Rev. D **78**, 034007 (2008), arXiv:10.0805.3653[hepph]

[14] Y.-R. Liu, X. Liu, W.-Z. Deng *et al.*, Eur. Phys. J. C **56**, 63 (2008), arXiv:10.0801.3540[hep-ph]

[15] Z.-S. Chen, Z.-F. Zhang, Z.-R. Huang *et al.*, JHEP **12**, 066 (2019)

[16] D. Harnett, R. T. Kleiv, K. Moats *et al.*, Nucl. Phys. A **850**, 110 (2011), arXiv:10.0804.2195[hep-ph]

[17] A. Palameta, J. Ho, D. Harnett, and T. G. Steele, Phys. Rev. D **97**, 034001 (2018), arXiv:10.1707.00063[hep-ph]

[18] A. Palameta, D. Harnett, and T. G. Steele, Phys. Rev. D **98**, 074014 (2018), arXiv:10.1805.04230[hep-ph]

[19] Z.-G. Wang and T. Huang, Eur. Phys. J. C **74**, 2891 (2014), arXiv:10.1312.7489[hep-ph]

[20] Z.-G. Wang, Eur. Phys. J. C **74**, 2963 (2014), arXiv:10.1403.0810[hep-ph]

[21] Q.-R. Gong, Z.-H. Guo, C. Meng *et al.*, Phys. Rev. D **94**, 114019 (2016), arXiv:10.1604.08836[hep-ph]

[22] R. M. Albuquerque and R. D. Matheus, Nucl. Part. Phys. Proc. **258-258**, 148 (2015)

[23] C.-Y. Cui, Y.-L. Liu, and M.-Q. Huang, Eur. Phys. J. C **73**, 2661 (2013), arXiv:10.1308.3625[hep-ph]

[24] W. Chen, T. G. Steele, M.-L. Du *et al.*, Eur. Phys. J. C **74**, 2773 (2014), arXiv:10.1308.5060[hep-ph]

[25] W. Chen, T. G. Steele, H.-X. Chen *et al.*, Phys. Rev. D **92**, 054002 (2015), arXiv:10.1505.05619[hepph]

[26] X. Liu, Z.-G. Luo, Y.-R. Liu *et al.*, Eur. Phys. J. C **61**, 411

(2009), arXiv:10.0808.0073[hep-ph]
[27] Y. Dong, A. Faessler, T. Gutsche *et al*., Phys. Rev. D **79**, 094013 (2009), arXiv:10.0903.5416[hep-ph]
[28] R. D. Matheus, F. S. Navarra, M. Nielsen *et al*., Phys. Rev. D **80**, 056002 (2009), arXiv:10.0907.2683[hep-ph]
[29] J. D. Jackson, Phys. Lett. B **87**, 106 (1979)
[30] Z.-G. Wang, Chin. Phys. C **41**, 083103 (2017), arXiv:10.1611.03250[hep-ph]
[31] Z.-G. Wang, Eur. Phys. J. C **78**, 518 (2018), arXiv:10.1803.05749[hep-ph]
[32] M. A. Shifman, A. I. Vainshtein, and V. I. Zakharov, Nucl. Phys. B **147**, 385 (1979)
[33] M. A. Shifman, A. I. Vainshtein, and V. I. Zakharov, Nucl. Phys. B **147**, 448 (1979)
[34] J. Ho, R. Berg, W. Chen, D. Harnett *et al*., Phys. Rev. D **98**, 096020 (2018), arXiv:10.1806.02465[hep-ph]
[35] S. Narison, Phys. Lett. B **675**, 319 (2009), arXiv:10.0903.2266[hep-ph]
[36] Z. Mo, C.-Y. Cui, Y.-L. Liu *et al*., Commun. Theor. Phys. **61**, 501 (2014), arXiv:10.1403.6906[hep-ph]
[37] R. D. Matheus, F. S. Navarra, M. Nielsen *et al*., EPJ Web Conf. **3**, 03025 (2010)
[38] A. Hart, C. McNeile, C. Michael *et al*. (UKQCD), Phys. Rev. D **74**, 114504 (2006), arXiv:10. heplat/0608026
[39] S. Narison, N. Pak, and N. Paver, Meson - Gluonium Mixing From QCD Sum Rules, 77 (1984)
[40] L. J. Reinders, H. Rubinstein, and S. Yazaki, Phys. Rept. **127**, 1 (1985)
[41] S. Narison, SVZ sum rules : 30 + 1 years later, Nucl. Phys. B Proc. Suppl. **207-208**, 315 (2010), arXiv: 1010.1959[hep-ph]
[42] J.-R. Zhang and M.-Q. Huang, Commun. Theor. Phys. **54**, 1075 (2010), arXiv:10.0905.4672[hep-ph]
[43] S. H. Lee, K. Morita, and M. Nielsen, Nucl. Phys. A **815**, 29 (2009), arXiv:10.0808.0690[hep-ph]
[44] M. Nielsen, F. S. Navarra, and S. H. Lee, Phys. Rept. **497**, 41 (2010), arXiv:10.0911.1958[hep-ph]
[45] F.-K. Guo, C. Hanhart, U.-G. Meißner *et al*., Rev. Mod. Phys. **90**, 015004 (2018), arXiv:10.1705.00141[hep-ph]